

Aeroacoustics of Aircraft Cavities

S. Crook¹, R. Kelso², J. Drobnik³

^{1,2}School of Mechanical Engineering,
 The University of Adelaide, South Australia, 5005, AUSTRALIA

³Air Vehicle Division, Defence Science and Technology Organisation (DSTO),
 Fishermans Bend, Victoria, 3207, AUSTRALIA

Abstract

The purpose of this study is to determine the aeroacoustic and fluid-dynamic nature of the flow field in and around a generic aircraft cavity in order to characterise the physical mechanism of noise and vibration generated by the flow. This paper discusses the experimental investigation of a narrow, shallow, rectangular cavity in both wind and water tunnel facilities. The experimental investigation primarily focuses on boundary layer characteristics, surface pressure distributions and surface flow visualisation. Qualitative and quantitative results are discussed.

This paper reports results for cavities of length:depth:width ratios of 6:1:2. The principal findings are in agreement with an "open" type flow as stated in the literature, however the flow within the cavity is highly three-dimensional in contrast with the suggestions of Stallings & Wilcox (1987). Significant three-dimensionality is also evident downstream of the cavity, close to the trailing edge. Further findings suggest the shear layer impinges below the edge of the rear wall in the mean, leading to a net inflow of free-stream fluid into the cavity at the centre line, which is balanced by an outflow adjacent to the side walls. Finally, a number of vortices are present at the rear wall, including a corner vortex at the base of the rear wall, and a vortex associated with flow separation on the trailing board adjacent to the rear wall edge.

Introduction

Aeroacoustic phenomena are of growing concern on air, ground and space vehicles. In particular, continuing advancement and modifications of aircraft and spacecraft are required in order to meet stringent noise certification requirements, to increase structural longevity and to control the local aerodynamic environment. Examples of this include the desire to stow weapons in cavity-type bays to increase stealth, and control of the flow field in and around exposed openings of airborne observatories [2].

This subject has numerous applications across many engineering fields, but a complete complex and three-dimensional fluid-dynamic study has not been undertaken in any great detail for narrow, long cavities at low velocities (~25m/s). Many two-dimensional studies have provided valuable 'grass-roots' theories, however the literature is limited and sometimes contradictory.

Aircraft Context

Over the years many aircraft have been developed with varying methods of weapons storage. It had been shown that external weapons carriers are responsible for increased radar cross-section and up to 30% of the total aircraft drag [11]. Motivated by these considerations, efforts to improve aircraft and stealth technology have led to the desire to stow weapons in an internal cavity-type bay. Unfortunately internal weapon bays have a number of disadvantages with the three main problems being 1) store damage; 2) stealth of aircraft (sound pressure levels); and 3) store release trajectory prediction [3, 12, 13, 14]. Firstly, the

stores and internal equipment housed within the cavity as well as jeopardising the cavity structure itself. Excessive structural vibrations may occur if the acoustic frequency matches the characteristic structural frequency of the cavity. Secondly, noise control is necessary for certain aircraft and with sound pressure levels as high as 180dB [5] the aircraft's level of stealth is greatly reduced. In addition, the personnel exposed to these high sound pressures may sustain considerable hearing damage. Finally, the ability to accurately predict trajectories followed by stores released from weapons bays of aircraft is crucial to the safety of Australian Defence Force (ADF) aircraft and personnel.

The cavities focused on in this investigation are modelled around a typical ADF aircraft weapon bay whose length-to-depth ratio (l/d) is approximately six and width-to-depth ratio (w/d) is approximately two (Figure 1). Considering the transonic and supersonic flow speeds achieved by the aircraft and the relatively low l/d ratios of its internal bay, it is shown (through past two-dimensional analysis) that the cavity experiences an open-type flow field as shown in Figure 2. In order to model this high-speed open cavity flow field using low subsonic conditions a maximum $l/d < 7$ would be needed to avoid transition into the closed cavity flow field [10]. Since many aircraft have l/d less than 7 it is reasonable to assume that the flow field will be completely open and hence allow a comparison of high speed open flows fields with low speed models. Of course other factors such as Reynolds number, boundary layer thickness and oscillation threshold are taken into account when modelling these high-speed flows.

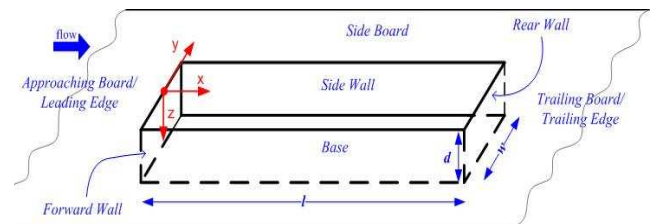


Figure 1 Cavity Nomenclature.

Cavity Classification and Flow Dynamics

Under certain fluid-cavity interactions the fluid-dynamic environment will generate periodic fluctuations that are detectable as audible tones and/or broadband noise. From an acoustic point of view the cavity is characterised by the nature of flow-induced resonance and large amplitude tones [7]. One of the main contributing factors to the nature of noise generation is the cavity geometry which is primarily defined in terms of length-to-depth ratios. This ratio can then be used to classify the fluid-dynamic environment as either being open (Figure 2a), closed (Figure 2b) or transitional. The l/d value at which the flow field switches from open to closed flow is termed the critical length-to-depth, l/d_{cr} .

Studies of two-dimensional cavity flow have shown that cavities with a low length-to-depth ratio (short and/or deep) have an open type flow, and those with higher length-on-depth ratios (long and/or shallow) tend to have closed flow fields. The critical length to depth ratio is dependent on a number of factors

the strongest being free stream flow velocity, U_∞ , and width-to-depth ratio, w/d . Pressure distribution experiments have shown that the critical division between open and closed flow at *supersonic* speeds is $l/d_{cr} < 11$ (open) and $l/d_{cr} > 11$ (closed) [4]. However a number of subsequent studies [14, 15, 16,] give a slightly different critical value due to the consideration of transitional flows: $l/d_{cr} \leq 10$ (open), $l/d_{cr} \geq 13$ (closed). At low *subsonic* speeds the boundary was found to be approximately $l/d_{cr} = 7-8$ [10].

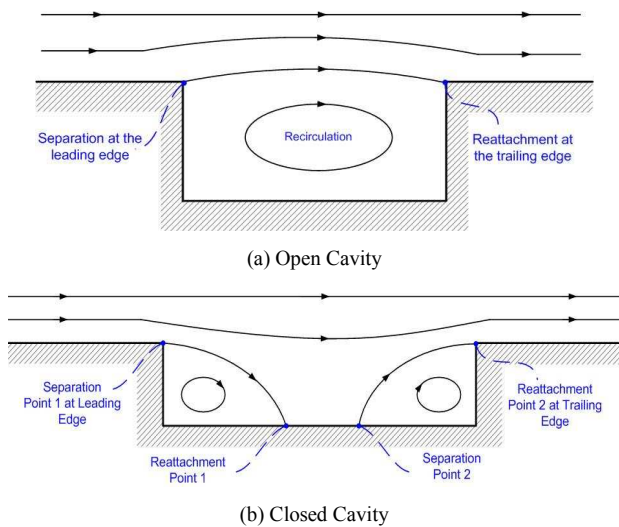


Figure 2 Cavity flow fields (2D simplified representation).

The second important fact that needs to be considered is the width of the cavity. Stallings & Wilcox (1987) studied the pressure distribution along the cavity floor centreline for a constant length and depth with varying widths. As the cavity width decreases the flow switches from transitional-open to transitional-closed flow. Further decrease of the width results in a closed flow field. The dividing value for open flow to closed flow for the width to depth ratio at supersonic speeds according to Stallings & Wilcox (1987) is approximately $w/d_{cr} < 1$ (open), $w/d_{cr} > 5$ (closed). In addition, as the cavity width decreases the critical l/d_{cr} value is lowered.

These studies illustrate the importance of taking into account the highly three-dimensional character of cavity flows.

Three-Dimensionality

The three-dimensionality of the flow field is an important issue when dealing with relatively narrow cavities. Stallings & Wilcox (1987) and later Wilcox (1990) investigated the three-dimensionality by measuring the lateral pressure gradients across the rear face of a cavity at supersonic flow speeds. It was found that for closed cavity flow the gradients are caused by the formation of vortices along the side walls as the flow expands into the cavity near the leading edge. For open flow fields, large lateral pressure gradients occur although the magnitudes are considerably less than for closed cavity flow. The results indicate that for the open flow field the side wall vortices are absent, making the three-dimensionality of the flow field much less complex than in closed flow fields. Hence, the effects of cavity width on the pressure distribution for open cavity flow fields are relatively small compared with those for cavities with closed flows. Increasing the width for open flow fields generally results in an increase in pressure on the cavity's rear face and on the rear portion of the cavity floor.

Research Objectives

The three-dimensional cavity flow description reported in literature is vague and the oscillation mechanism is generally adapted from the simplified two-dimensional version, which is inadequate for relatively narrow cavities.

The key objectives of the current research are:

- To develop an understanding of cavity flow fields of narrow, three-dimensional, open-type cavities with slightly differing geometries (length : depth : width ratio);
- To explore means to alleviate and control the undesirable effects such as high acoustic loading and attempt to translate these results to higher Mach number flows.

Experimental Equipment and Methodology

A series of preliminary wind and water tunnel visualisation tests were conducted on the surface and within the volume of the cavity. The aim of the preliminary tests was to determine regions of particular interest, such as high pressures, high turbulence or vortical structures. These regions could then be quantitatively investigated in more detail using time-averaged surface pressure data.

Surface pressure and boundary layer measurements were taken upstream of the cavity in order to assess the quality of the wind tunnel flow, such as the velocity profile and spanwise uniformity at wind tunnel exit, and boundary layer characteristics (thickness, uniformity and turbulence).

Cavity Geometry and Model Considerations

The standard cavity test rig was based on a 1/10th scale model of an ADF aircraft. The standard geometric case consists of $l/d=6$, which by all definitions is an open type cavity configuration regardless of the free stream Mach number. Modifications to the $l/d/w$ ratio have been carried out to investigate the effects of increasing the three-dimensionality of the flow field. The cavity geometries under investigation include $l/d/w$ ratios of: Case A-6:1:2, Case B-6:1:1.5 and Case C-6:1:1. (Case B and Case C results are not presented in this paper).

The model (Figure 3) is free standing and separated from the wind tunnel walls. The advantage of this is that the boundary layer characteristics are a result of flow over the model only and not the cumulation of flow through the tunnel ducting. This allows greater control over the boundary layer characteristics. The leading edge of the plate is super-elliptic [8] and a thin trip was installed to generate a turbulent boundary layer of the desired thickness.



Figure 3 Cavity model with tunnel's side walls and roof removed.

The leading edge spanwise uniformity was confirmed through measurements of boundary layer thicknesses at various positions across the width of the cavity as well as the spanwise pressure distribution.

The trailing edge of the model was designed to have an adjustable spoiler such that stagnation at the tip of the super-ellipse leading edge was achieved. The spoiler and a mesh screen attached to the tunnel enclosure were used to offset blockage caused by the protruding underside of the model.

Free Stream Flow Conditions

Velocities are chosen to allow adequate measurements, visualisation and control of primary characteristics which are important for comparing fluid-dynamic resonance with the full-scale aircraft. The flow cases considered are:

- Wind Tunnel @ 25m/s, 20m/s
- Water Tunnel @ 0.6m/s

The desired conditions were achieved by optimising the free stream velocity (Reynolds number), the contour of the super-elliptic leading edge and its distance from the cavity, the position and diameter of the boundary layer trip, and the location of the leading edge stagnation point. It was necessary to investigate the development of the boundary layer upstream of the cavity in order to identify any instability.

The boundary layer thickness was measured at the leading edge of the cavity using a miniature Pitot-static tube with 0.4mm internal diameter. The probe was traversed with a step size of 0.2mm through the boundary layer into the free stream. Proximity corrections and wall shear stress corrections were applied to these readings [6]. In addition, there was a requirement to maintain a constant velocity region, wide enough to cover the cavity with an effectively constant free stream velocity. In a free jet, an acceptable velocity variation is achieved when the total pressure varies by less than 1% which corresponds to a velocity variation of less than 0.5% [1]. The 1% pressure variation criterion was applied to spanwise surface pressure leading up to the cavity opening as well as boundary layer thickness variation across the width of the cavity at the leading edge.

Flow Visualisation

Flow visualisation was used to identify features of the flow such as streak line patterns, impingement regions and separation zones. It also gave a global indication of flow development and fluid-dynamics of the system to identify areas of interest for future tests.

Surface Tuft Flow Visualisation and Surface Paste Visualisation (air) preliminary experiments were carried out at a Reynolds Number (based on free stream velocity and cavity length) of $\sim 1 \times 10^5$ and boundary layer thickness of ~ 15 mm at the leading edge cavity corner. Video and still imaging were used for visual analysis. Tuft length was 40mm with a tuft grid spacing 60mm streamwise for the length of the cavity and 40mm spanwise for the width of the cavity. Visualisation was also conducted using a hand-held probe and was used to confirm the presence of many of the flow features observed using other techniques.

A small number of **Volumetric Dye Visualisation** (water) experiments were conducted using the facilities located at DSTO (Melbourne). Images were captured on both video and still digital cameras. All tests were conducted at a free stream velocity of 60mm/s with a leading edge length of 290mm, Reynolds Number $\sim 1.5 \times 10^4$ and boundary layer thickness ~ 12 mm at the leading corner.

The dye was injected at both the leading wall and the rear wall and illuminated by a light sheet which could be moved to any position along the width of the cavity.

Surface Pressure Measurements (Air)

A total of 192 pressure ports were installed into the cavity and its surrounding board in a grid pattern. These ports were scanned using four-48-port Scani-Valves. Each port has a diameter of 0.4mm.

The separations between ports varied depending on their location. For instance, the forward region of the cavity was shown to have very low pressure variation and was of little interest when viewed using surface flow visualisation. Therefore, the forward region contained relatively few ports, whereas the region of greatest interest, the rear of the cavity, contains a greater number of ports with a smaller separation. Each set was run three times to ensure the results were repeatable. Results were split into seven geometric regions for analysis. The pressure port grid pattern (spatial resolution) and geometric size for each of these regions are given in the following table:

	Lengthwise (x-axis)	Spanwise (y-axis)	Depthwise (z-axis)
Approaching Board (L=450mm)	80-200mm	38-150mm	
Forward Wall (d=75mm, w=150mm)		37.5mm	18mm
Side Wall (l=450mm, d=75mm)	50mm		18mm
Rear Wall (d=75mm, w=150mm)		37.5	18mm
Base (l=450mm, w=150mm)	50mm	37.5mm	
Side Board (w=150mm)	50mm	20mm	
Trailing Board (L _{TB} =950mm)	50mm	37.5mm	

Table 1 Location and separation of pressure ports for $l/d=6$, $w/d=2$.

Pressure was measured on a 10Torr Baratron and digitally displayed on a MKS signal conditioner. The output was recorded on a National Instruments USB-6009 Data Logger and DAQmx Base Software. The timing between scans and data recording was controlled using a standard signal generator. Each port was sampled at 1000Hz for 60seconds. Post processing of the data was carried out using MATLABTM. Resulting pressure distributions are shown in Figure 8.

The systematic and random errors associated with the above measurements amount to a total error in the order of ± 0.010 Pa, or 0.05% in the worst case. Other associated errors may include misalignment of the Pitot-static tube and the formation of a stagnation point within the pressure port opening. The Pitot tube was carefully positioned reducing the misalignment to the order of 1-2degrees, which according to Ower and Pankhurst [9] is acceptable to provide a true reading of the free stream pressure.

Results

Surface Tuft Visualisation (air)

Tuft flow visualisation indicated a definite recirculation region inside the cavity, with the strongest reversed flow occurring toward the rear wall ($\approx 4l$). The tufts showed that along the sides of the cavity there is some weak lateral flow into the cavity on the forward part and then stronger lateral flow out of the cavity towards the rear. At the rear wall the flow appeared to be highly turbulent. Some vortical features were also noted on the internal and external surfaces at the rear of the cavity.



Figure 4 Photo of tuft flow visualisation experiments. Free stream flow from right to left.

Surface Paste Visualisation (air)

Paste visualisation revealed a number interesting features that were not obvious in the tuft experiments. The pattern confirmed the presence of a strong recirculation towards the rear of the cavity, and also a number of flow features at the rear of the cavity. These include a number of separation and reattachment lines both at the junction between the base and the rear wall (consistent with a small spanwise corner vortex) and between the rear wall and the trailing board (consistent with a zone of separation downstream of the cavity trailing edge). A typical flow pattern and an interpretation are presented in Figure 6. The present features are indicated by blue dashed lines. In addition, a pair of spiral-like surface features were evident on the base at the downstream corners of the cavity, indicating the existence of vortical features in this region. The paste patterns also revealed a significant region of outflow over the sidewall edges at the rear of the cavity. Investigation with a hand-held tuft probe showed that a stream wise vortex is present in this outflow region. A proposed time-average flow pattern is shown in Figure 6.

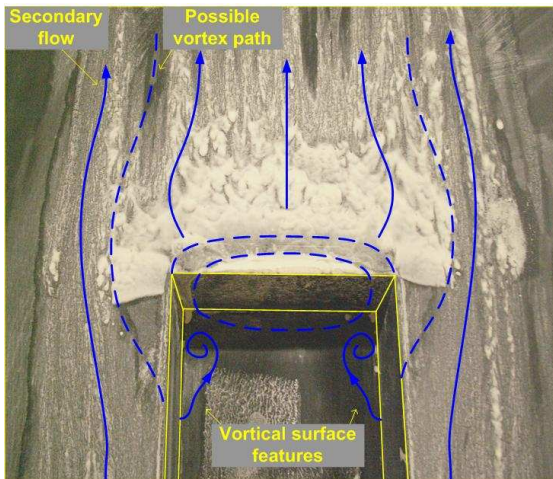


Figure 5 Rear trailing edge (looking down), $l/d=6$ and $w/d=2$.

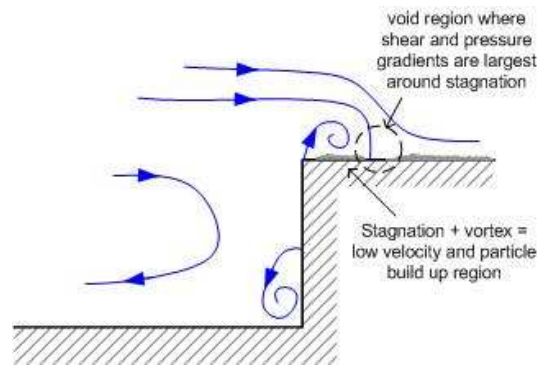


Figure 6 Proposed time-average flow pattern developed from experimental observations – 2D representation of centre line, $l/d=6$ and $w/d=2$.

Dye visualisation (water)

Observations of the video images showed a quasi-periodic roll up of the shear layer over the cavity. The shear layer was observed to impinge on the rear wall, with the impingement point flapping such that the shear layer material was either recirculated into the cavity, or flowed over the downstream lip. The middle and downstream regions of the cavity were seen to be highly intermittent and turbulent. At the junction between the base and the rear wall a corner vortex was observed consistently, as shown in Figure 7c. This observation agrees well with previous surface flow visualisation results.

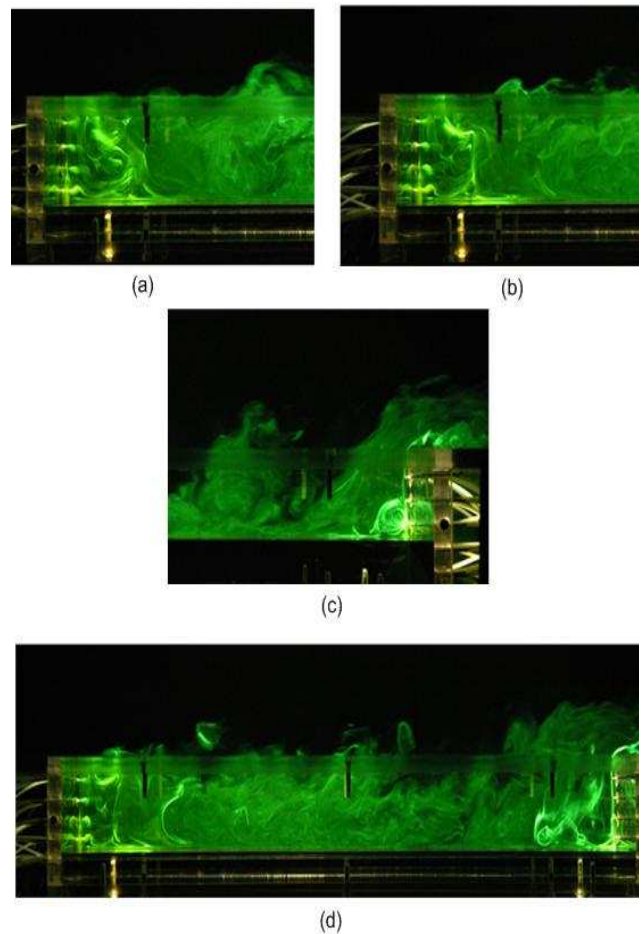


Figure 7 Images of dye flow visualisation taken during preliminary experiments, light sheet along centreline for a cavity of $l/d=6$ and $w/d=2$: a) & b) forward region, c) small vortex formed in the rear corner, d) typical flow field.

Scani-Valve Surface Pressure Results

Approaching board and **forward wall** results show a highly uniform spanwise surface pressure which varied less than 1% for all tests. The streamwise pressure along the approaching board was seen to increase slightly in the downstream direction creating a small but favourable pressure gradient, again less than 1% variation was recorded. The lack of variation and relatively low pressure on the forward wall supports previous results.

The leading edge spanwise uniformity was supported through measuring and comparing boundary layer thicknesses at various positions across the width of the cavity. The average boundary layer thickness for 25m/s free stream flow was 9.3mm and for 20m/s it was 9.9mm. The boundary layer was tripped at the leading edge of the model to create a turbulent profile which was comparable to the full size aircraft simulations.

Results for both the **side wall** and **base** are remarkably similar. They both indicate a decreasing pressure from the forward wall through to $\frac{3}{4}$ of cavity length. The pressure then dramatically rises to a maximum level at the rear of the cavity. Spanwise pressure along the base of the cavity varied only slightly, having a lower centre pressure and a higher pressure towards the side walls. Spanwise symmetry was also very strong for the entire length of the cavity base.

The **rear wall** spanwise pressure distribution is, as expected, symmetric about the centre line. This rear wall exhibits the maximum pressure seen throughout the cavity, being approximately 80% of the free stream total pressure. The maximum is seen close to the rear lip of the cavity trailing edge along the centre line. The surface pressure pattern on the rear wall also reveals two distinct low pressure regions.

Interestingly, the **rear board** shows a dramatic drop in pressure downstream of the cavity edge, with the largest change occurring on the centreline of the cavity. The pressure then rises rapidly downstream of the edge.

Discussion

The wool tuft, paste and dye visualisation studies all indicate that the flow pattern formed within the present cavity is of "open" type, in agreement with the literature. However, in contrast to the schematic representation of Figure 2 (a), the recirculation of the flow is strongest at the rear of the cavity, with the centre of the mean recirculation at approximately $\frac{3}{4}l$ downstream from the forward wall. The flow visualisation and pressure distribution studies all indicate considerable secondary flow within the cavity, as will be discussed.

Figure 9 shows a schematic representation of the time-averaged flow pattern that occurs in the shear layer impingement region at the rear of the cavity, based on the flow visualisation observations made thus far. This pattern is representative for most of the cavity span, excluding the regions near the side walls. Clearly, the shear layer vortices impinging on the rear wall lead to a significantly more complex pattern at any instant in time, one effect being the oscillation of the

stagnation/bifurcation line. The main features of this region will now be discussed.

In order to satisfy conservation of mass within the cavity, there must be, on average, equal inflow and outflow of fluid. Both the surface tuft visualisation (hand-held probe) and the pressure distributions (Figure 8) showed that the shear layer over the cavity opening impinged below the lip of the rear wall. The total pressure at the stagnation point on the centre line is around 80% of the free stream total pressure, which implies that there is a significant flow of high-momentum fluid entering the cavity beneath the reattachment zone. Together, these results imply that the shear layer impingement leads to a net inflow of fluid into the cavity. Consistent with this, the tuft studies and the dye visualisation indicated that there is an outflow of fluid from the cavity along the downstream surfaces of the side wall. Surface tuft and paste visualisation studies indicated the presence of some complex vortical feature in the surface flow in this region (Figure 5), but the features could not be fully resolved.

Surface paste visualisation also indicates the presence of vortical features on the cavity base near the junction with the side and rear walls (Figure 5). These features correspond to features of similar size in the surface pressure patterns (Figure 8), although the pressure port spacing was not sufficiently fine to resolve any details. In addition, water-based dye visualisation showed the presence of a spanwise "corner" vortex at the junction of the base and rear wall (Figure 6) and this is consistent with the surface streak pattern obtained using the paste visualisation in air (Figure 5).

An interesting feature of the pressure distributions (Figure 8) is the pair of low-pressure peaks on the rear wall. These peaks do not correspond to any features detected during any of the flow visualisation experiments. However, during experiments with a hand-held tuft probe, it was observed that the impingement of the shear layer on the rear wall was further from the cavity edge and fluctuated more at the centre line than at the sides of the cavity. Thus, it is proposed that the double-peak character of the rear wall pressure distribution is a result of the curvature and increased oscillation of the impinging shear layer at the centre line, rather than indicating any significant flow feature.

Finally, the presence of a region of separation on the trailing board adjacent to the rear wall edge, was strongly evident in the dye visualisation, the paste and tuft visualisation experiments, and also in the pressure distributions. The flow pattern in Figure 9 reconciles these observations. The main feature is the separation and roll up of the shear layer flowing from the rear wall to form a small vortex above the cavity edge. Beneath this vortex there is reversed flow, corresponding to a low pressure region. Significant amounts of paste also accumulate beneath this vortex. Downstream of this vortex, there is a flow reattachment, corresponding to a void in the paste distribution, then forward (streamwise) flow further downstream. Of particular note is the spanwise variation in the pressure distribution (Figure 8) and the curvature of the reattachment line (Figure 9), both of which indicate significant three-dimensionality of the flow close to the cavity trailing edge.

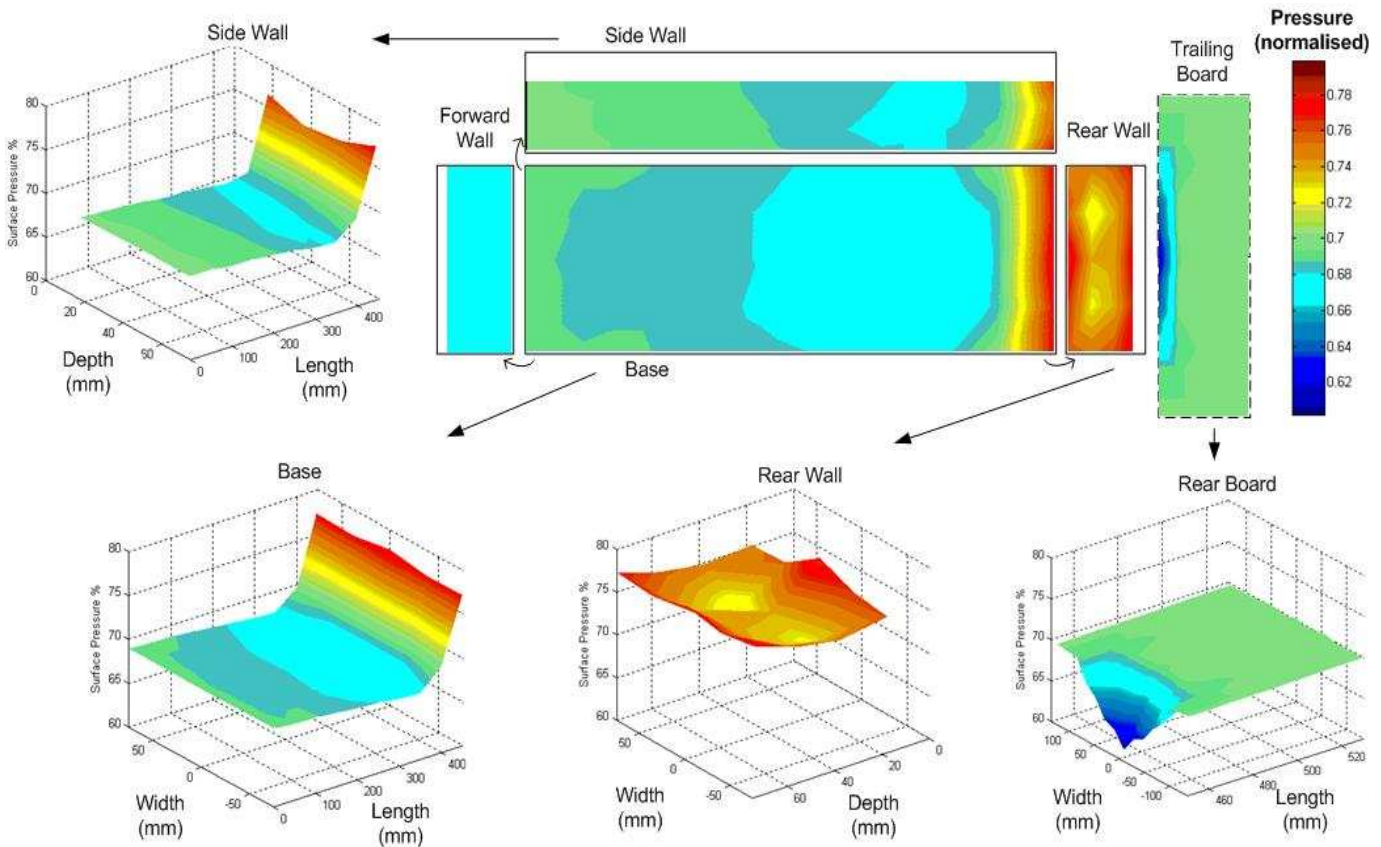


Figure 8 Surface pressure distribution, normalised against free stream stagnation pressure, $l/d=6$ & $w/d=2$.

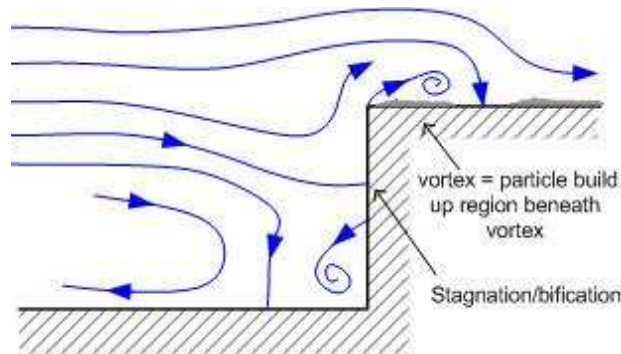


Figure 9 New proposed time-average flow pattern based on surface pressure experiments, $l/d=6$ and $w/d=2$.

Conclusion

Observing the flow within and around the cavity revealed the existence of a highly three-dimensional field. These observations agree well with the early assessment that the current two-dimensional simplified description in the literature (Figure 2) is not adequate to accurately and fully describe the flow field. In particular, the rear region of the cavity is complex and unsteady, and requires further analysis to be fully understood.

The key conclusions of this work are:

- The flow pattern formed within the present cavity is of "open" type, in agreement with the literature.
- The flow within the cavity is highly three-dimensional, in contrast with the suggestions of Stallings & Wilcox (1987). Significant three-dimensionality is evident downstream of the cavity, close to the training edge.

- The shear layer above the cavity impinges below the edge of the rear wall in the mean, leading to a net inflow of free-stream fluid into the cavity at the centre line, which is balanced by an outflow adjacent to the side walls.
- A number of vortices are present at the rear wall, including a corner vortex at the base of the rear wall, and a vortex associated with flow separation on the trailing board adjacent to the rear wall edge.

Comparison of the pressure distribution with the surface flow pattern has allowed a more detailed description and analysis of the surface flow topology. In addition, contours of surface pressure assist in ascertaining quantitatively the effect of geometry on the three-dimensionality of the flow.

Future Work

Future work includes additional surface pressure investigation for cavity geometry based on Case B (6:1:1.5) and Case C (6:1:1). This will provide further three-dimensional information.

To compliment these results, further visualisation tests will be carried out in a water tunnel. These will include dye flow visualisation and Particle Image Velocimetry across the volume of the cavity.

Acknowledgements

The authors would like to express thanks to Eyad Hassan, Tim Lau, Peter Lansberry and Paul Medwell for their time and advice. Authors are also grateful to the electronic staff and workshop staff, School of Mechanical Engineering, The University of Adelaide for providing technical assistance. Thanks must also be given to Defence Science and Technology Organisation for support and funding.

References

- [1] Ahuja, K. K. & Mendoza, J. M., *Effects of Cavity Dimensions, Boundary Layer and Temperature on Cavity Noise with Emphasis on Benchmark Data to Validate Computational Aeroacoustic Codes*, NASA Langley Research Centre, Hampton, VA, 1995
- [2] Atwood, C. A., Selected Computations of Transonic Cavity Flows, *Computational Aero- and Hydro-Acoustics, ASME 1993, (FED-Vol) 147*, 1993 7-18
- [3] Blair, A. B., Jr., & Stallings, R. L., Jr., Supersonic Axial-Force Characteristics of a Rectangular-Box Cavity With Various Length-to-Depth Ratios in a Flat Plate, *NASA TM-87659*, 1986
- [4] Charwat, A. F., Foos, J. N., Dewey, F. C. & Hitx, J. A., An Investigation of Separated Flows -Part 1: The Pressure Field, *Journal of Aerospace Sciences*, **28(6)**, 1961 457-70
- [5] Larcheveque, L., Saguat, P. & Le, T.-H., Large Eddy Simulation of flows in Weapons bay, *AIAA*, 2003
- [6] McKeon, B. J., Li, J., Jiang, W., Morrison, J. F. & Smits, A. J., Pitot Probe Corrections in Fully Developed Turbulent Pipe Flow, *Measurement Science and Technology*, **14**, 2003 1449-1458
- [7] Milbank, J., Investigation of Fluid-Dynamic Cavity Oscillations and the Effect of Flow Angle in an Automotive Context using an Open-Jet Wind Tunnel, RMIT University, Melbourne, Australia, 254, 2004
- [8] Narasimha, R. & Prasad, S., Leading Edge Shape for Flat Plate Boundary Layer Studies, 1994
- [9] Ower, E. & Pankhurst, R., *The Measurement of Air flow*, Pergamon Press Ltd., Oxford, 1966
- [10] Sarohia, V., Experimental Investigation of Oscillations in Flows Over Shallow Cavities, *AIAA Journal*, **15(7)**, 1977 984-91
- [11] Shaw, L., Bartel, H. & McAvoy, J., Acoustic Environment in Large Enclosures with a Small Opening Exposed to Flow, *Journal of Aircraft*, **30(3)**, 1982 250-256
- [12] Stallings, R. L., Jr, Wilcox Jr, F., Blair, A. B., Jr & Monta, W. J., *Store Carriage Drag and Separation at Supersonic Speeds*, Langley Symposium on Aerodynamics, **2**, 1986 251-268
- [13] Stallings, R. L., Jr., Store Separation From Cavities at Supersonic Flight Speeds, *J. Space & Rockets*, **20**, 1983 129-132
- [14] Stallings, R. L., Jr, & Wilcox, F., Jr, Experimental Cavity Pressure Distributions at Supersonic Speed, *Langley Research Centre Hampton, Virginia; NASA Technical Paper 2683*, 1987
- [15] Tracy, M. & Plentovish, E., *Characterization of Cavity Flow Fields Using Pressure Data Obtained in the Langley 0.3-Meter Transonic Cryogenic Tunnel*, *NASA Technical Memorandum 4436*, Langley Research Centre, Hampton, Virginia, 1993
- [16] Wilcox Jr, F., *Experimental measurements of Internal Store Separation Characteristics at Supersonic Speeds*, Store Carriage, Integration and Release Conference, 1990 5.1-5.16